Synthesis, Morphology, and Mechanical Properties of Poly(methyl methacrylate)-*b*-poly(*n*-butyl acrylate)-*b*-poly(methyl methacrylate) Triblocks. Ligated Anionic Polymerization vs Atom Transfer Radical Polymerization

J. D. Tong,[†] G. Moineau,[†] Ph. Leclère,[‡] J.L. Brédas,[‡] R. Lazzaroni,[‡] and R. Jérôme*,[†]

Center for Education and Research on Macromolecules (CERM), University of Liège, Sart-Tilman, B6, B-4000 Liège, Belgium, and Service de Chimie des Matériaux Nouveaux, Centre de Recherche en Electronique et Photonique Moléculaires, Université de Mons-Hainaut, Place du Parc 20, B-7000 Mons, Belgium

Received June 3, 1999

ABSTRACT: Poly(methyl methacrylate)-*b*-poly(*n*-butyl acrylate)-*b*-poly(methyl methacrylate) triblock copolymers have been prepared by ligated anionic polymerization (LAP; 8K-50K-8K) and atom transfer radical polymerization (ATRP; 9K-51K-9K). Size exclusion chromatography, nuclear magnetic resonance, and differential scanning calorimetry have confirmed that the molecular structure of the two triblock copolymers is essentially identical. However, important differences are found in dynamic mechanical properties, viscoelastic properties, and stress−strain behavior. Indeed, the ATRP copolymer has low storage modulus, high complex viscosity, high order−disorder transition temperature, and poor ultimate tensile strength and elongation at break, compared to those of the LAP analogue. Marked differences also observed by tapping mode atomic force microscopy in the microscopic morphology of thin films of these copolymers. All these observations can be explained by the slow initiation of MMA by the poly(*n*-butyl acrylate) macroinitiator used in ATRP in contrast to what happens when MMA is added to living poly-(*tert*-butyl acrylate) anions. As a result, the polydispersity of the short poly(methyl methacrylate) (PMMA) outer blocks is much broader in the ATRP copolymer, although the polydispersity index of the triblock is only 1.15. This heterogeneous structure of the ATRP triblock is also supported by the comparison of homo-PMMAs prepared by LAP and ATRP.

Introduction

The steadily increasing capability of ligated anionic polymerization (LAP) and atom transfer radical polymerization (ATRP) of (meth)acrylic monomers allows new polymeric materials of well-defined molecular structure to be synthesized.[1−4] Fully (meth)acrylic triblocks with a central rubbery poly(alkyl acrylate) block and outer hard poly(alkyl methacrylate) blocks are typical examples of possible substitutes for the traditional styrene−diene-based thermoplastic elastomers (TPEs); there is indeed a demand for improving the poor oxidation resistance and the relatively low service temperature (60−70 °C) of the polydiene-containing TPEs. Fully (meth)acrylic triblock copolymers have the advantage of covering a large range of glass transition temperatures (T_g) simply by changing the alkyl substituent of the ester group, e.g., from −50 °C for poly(isooctyl acrylate) up to 190 °C for poly(isobornyl methacrylate). Furthermore, immiscibility of alkyl polymethacrylates and polyacrylates is the rule, although some exceptions may be found in the case of small alkyl groups and low molecular weight (MW).[5] The much higher resistance of poly(meth)acrylates to UV and oxidation compared to that of polydienes is a substantial improvement.

Recently, we have synthesized PMMA-*b*-poly(*n*-butyl acrylate)-*b*-PMMA triblock copolymers (MnBM) by LAP[6] and ATRP.[7] The anionic synthesis of MnBM relies upon the three-step sequential polymerization of MMA, *tert*-butyl acrylate (tBA), and MMA, followed by the acid-catalyzed transalcoholysis of the *tert*-butyl ester groups by *n*-butanol. The radical synthesis requires that polymerization of *n*-butyl acrylate is initiated by a difunctional compound followed by polymerization of MMA. Although copolymers synthesized by LAP and ATRP may be of the same molecular structure (MW, MWD, and composition), the static and dynamic mechanical properties of the LAP-prepared triblock may be quite different from the counterpart prepared by ATRP. So the question is raised to know whether the origin for these important differences has to be found in the PMMA tacticity (thus in T_g of the hard microdomains), the extent of the phase separation, or the molecular characteristics of the constitutive blocks. This paper aims at addressing this issue by reporting on the synthesis of the same MnBM triblock by LAP and ATRP and on the molecular structure and properties of these two resulting copolymers. For this purpose, the glass transition temperatures (T_g) of the triblocks will be measured by differential scanning calorimetry (DSC), the phase morphology will be observed by atomic force microscopy (AFM), and the static (stress−strain curves) and dynamic mechanical properties will be analyzed, and all these observations will be discussed in close relation to the molecular structure of the triblocks previously analyzed by size exclusion chromatography and nuclear magnetic resonance.

Experimental Section

Materials. THF and toluene were dried by refluxing over the deep purple sodium benzophenone complex. MMA, tBA,

[†] University of Liège.
[‡] Université de Mons-Hainaut.
* To whom correspondence should be addressed.

and nBA (Aldrich) were refluxed over CaH₂, vacuum-distilled, and stored under nitrogen at −20 °C. Before anionic polymerization, MMA and tBA were added with 10 wt % AlEt₃ solution in hexane until a persistent yellowish-green color was observed and distilled under reduced pressure just prior to use. (tBA was diluted by the same volume of toluene before distillation.) *sec*-Butyllithium (*sec*-BuLi) (Aldrich, 1.3 M solution in cyclohexane) was diluted by cyclohexane (ca. 0.25 N). 1,1-Diphenylethylene (DPE, Aldrich) was vacuum-distilled over *sec*-BuLi and diluted by toluene (ca. 0.3 N). *n*-Butanol (Janssen) was used as received. LiCl (99.99%, Aldrich) was dried under vacuum at 130 °C. Toluene used for ATRP polymerization was degassed by bubbling N₂ for 20 min. NiBr₂(PPh₃)₂ (99%) and diethyl *meso*-2,5-dibromoadipate (98%) were used as received from Aldrich. NiBr₂(PPh₃)₂ was stored under nitrogen.

Anionic Synthesis of PolyMMA-*b*-polytBA-*b*-polyMMA (MTM) Precursors. A known amount of LiCl was added to a glass reactor previously flamed under vacuum and purged with nitrogen. THF and DPE were transferred into the glass reactor through rubber septa and stainless steel capillaries or syringes. A 3-fold molar excess of DPE and a 5-fold molar excess of LiCl were used with respect to *sec*-BuLi. The initiator solution was then added dropwise until a red color persisted, followed by the desired amount of initiator. The solution was then cooled to −78 °C and added with the required amount of MMA. The polymerization was conducted at −78 °C for 1 h. Upon MMA addition, the deep red color of the initiator immediately disappeared, indicating instantaneous initiation. The sequential addition and polymerization of tBA and MMA were carried out under the same experimental conditions. The copolymerization product was quenched by degassed methanol, and the final solution was concentrated before being precipitated into an excess of 90/10 (v/v) methanol/water mixture under stirring. The crude copolymer was dried under vacuum at 60−80 °C overnight.

Derivatization to Poly(MMA)-*b*-poly(nBA)-*b*-poly(MMA) (MnBM) Copolymers. On the basis of preliminary experiments, the best conditions for the transalcoholysis of the tBA units of MTM copolymers consisted in dissolving the copolymer in excess of *n*-butanol in the presence of *p*-toluenesulfonic acid (PTSA; 10 mol % with respect to tBA units). After reflux at 130 °C for 48 h, the copolymer was recovered by precipitation in methanol and dried under vacuum at 80 °C overnight.

ATRP Synthesis of α,ω-Dibromo-PnBA Macroinitiator. A 0.129 g sample of diethyl *meso*-2,5-dibromoadipate (0.358 mmol) and 0.266 g of NiBr₂(PPh₃)₂ (0.358 mmol) were introduced into a glass reactor equipped with a three-way stopcock and magnetic stirrer. Oxygen was removed by three vacuum−nitrogen cycles. A 30 mL aliquot of nBA (0.209 mol) was then added with a syringe, and the glass reactor was immersed in an oil bath at 85 °C. After 18 h, the reaction mixture was diluted by toluene, and the polymer was precipitated in methanol. The catalyst was removed by passing the PnBA toluene solution through an Al₂O₃-containing column. The α,ω-bromo-PnBA (51 000 MW) was recovered after drying overnight at 85 °C under high vacuum (73% conversion; 19.55 g).

ATRP Synthesis of MnBM Triblocks. The α,ω-bromo-PnBA macroinitiator (8 g) was dissolved in toluene (50 wt %), then introduced into a round-bottom flask, and degassed by nitrogen bubbling. Part of toluene was distilled off until the polymer concentration was ca. 50 wt %. NiBr₂(PPh₃)₂ (0.28 mol) was then added under nitrogen followed by MMA (3.6 mL). Polymerization was carried out at 85 °C and monitored by SEC and NMR until the required molecular weight (MW) was reached. The reaction mixture was then diluted by toluene, and the block copolymer was precipitated in methanol. It was further dissolved in toluene and purified by passing through an Al₂O₃ column in order to remove the catalyst. Finally, the MnBM triblock was dried under vacuum at 85 °C overnight.

Sample Preparation. Films were prepared by casting a copolymer solution (8 wt %; 160 mL) in toluene in 100 mm diameter polyethylene dish. The solvent was let to evaporate for 3−4 days at room temperature. Films were dried to

constant weight in a vacuum oven at 80 °C for ca. 1 day. They were colorless, transparent, and elastomeric with a smooth surface. For AFM measurements, the samples were prepared by solvent casting from 1 mg/mL solution in toluene on freshly cleaved muscovite mica substrates. The thickness of the films was ca. 400 nm, which makes the surface structure independent of the substrate and of possible interaction of components with it. They were annealed at 140 °C in a vacuum for 24 h prior to analysis.

Analysis. MW and MWD were measured by size exclusion chromatography (SEC) in THF with a Hewlett-Packard 1090 apparatus equipped with linear styragel columns. PMMA standards were used for calibration. The universal calibration by Benoit et al.[8] was used to calculate the MW of homo-PMMA and homo-PnBA, with the following viscosimetric relationships:

$$[\eta] = 1.298 \times 10^{-4}M^{0.688} \text{ (PMMA in THF)}^9 \qquad (1)$$

$$[\eta] = 7.4 \times 10^{-5}M^{0.75} \text{ (PnBA in THF)}^{10} \qquad (2)$$

¹H NMR spectra were recorded at 25 °C with a Bruker AM-250 spectrometer by using CDCl₃ as solvent and TMS as internal reference.

Dynamic mechanical and viscoelastic properties were measured with the RSI ARES rheometer from Rheometrics equipped with a force balance transducer. For temperature sweep experiments, 7 mm diameter samples were cut from 1 to 2 mm thick solution-cast films. They were tested in the shear mode (1 Hz frequency) at the 5 °C/min scanning rate. For frequency sweep experiments, parallel plate (25 mm diameter) and cone−plate (plate of 25 mm diameter, cone of 4° angle, and gap of 56 μm between the cone tip and the plate) were used for the analysis of triblock and homo-PMMA samples, respectively. The temperature control was accurate within 1 °C. The applied strain was kept within the linear viscoelastic regime, so that shear did not change the phase morphology. The experimental data were reproducible when repeated for samples prepared separately.

Tensile properties were measured with an Adamel Lhomargy tensile tester. Microdumbells were cut from solution-cast films and extended at 100 mm/min at room temperature. Sample thickness and width were 1.5 and 4 mm, respectively. At least three independent measurements were recorded for each sample.

The AFM measurements were performed in the "tapping mode". The cantilever holding the probe tip was oscillated at the resonance frequency (ca. 300 kHz) above the sample surface, so that the tip was in short-time contact with the surface at the lower end of the oscillation. This method minimized the amount of energy transferred from the tip to the sample compared to the contact-mode operation in which the tip was in permanent contact with the surface while scanning. The topography of the sample was recorded from the changes in the oscillation amplitude while performing a two-dimensional scan over the surface. Recently, the phase of the oscillating tip was observed to be very sensitive to the mechanical properties of the surface.[11] Therefore, the phase image recorded simultaneously to the amplitude image provides a map of the local mechanical properties and allows one-phase-separated microdomains to be observed. All the AFM images were recorded with a Nanoscope IIIa microscope from Digital Instruments Inc. operated at room temperature in air, using microfabricated cantilevers with a spring constant of 30 N m⁻¹. The instrument was equipped with the Extender TM Electronics module, such that height and phase cartographies could be recorded simultaneously. Several areas of the same sample were observed, with scanning times of ca. 5 min. The phase image was recorded in the so-called soft tapping mode, the ratio of the amplitude during measurement to the free amplitude, A_{sp}/A_0, being 0.95, to prevent deformation and indentation of the polymer surface by the tip. All the images were recorded with the maximum available number of pixels (512) in each direction. For image analysis, the Nanoscope
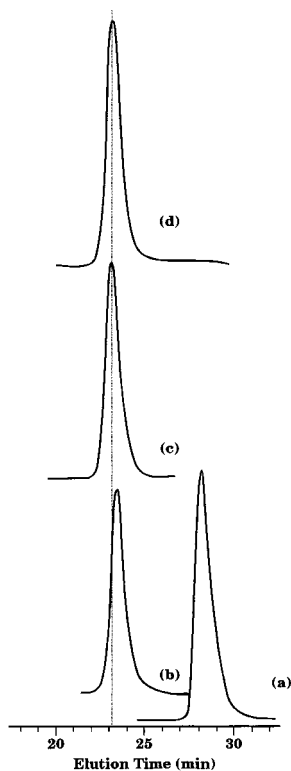
Figure 1. SEC traces of (a) PMMA first block, (b) PMMA-*b*-PtBA diblock, (c) PMMA-*b*-PtBA-*b*-PMMA triblock, and (d) MnBM triblock prepared by LAP.

Table 1. Characterization of the MnBM Triblock Copolymers

sample	M_n ($\times 10^{-3}$)	M_w/M_n	PMMA (wt %)	T_g of PMMA[a](°C)	T_g of PnBA[a] (°C)
1, LAP	8-50-8	1.05	24	107	−40
2, ATRP	9-51-9	1.15	26	105	−38

[a] DSC measurements.

image processing software was used. Unless otherwise mentioned, the images were not filtered and reported as captured. Repeated scans indicated that the observed structures were reproducible.

Results and Discussion

Anionic Synthesis of MnBM Triblock. Nucleophilic side reactions are known to perturb the anionic polymerization of primary acrylates even at low temperature. Although this situation is improved by the addition of a chelating $\mu-\sigma$ dual ligand, such as polydentate lithium alkoxide,[12] this improvement is not sufficient to allow well-defined MnBM triblocks to be synthesized, at least with high MW.[13] Therefore, the targeted MnBM triblock copolymer has been synthesized in an indirect way, i.e., sequential living anionic copolymerization of MMA, tBA, and MMA, followed by the selective acid-catalyzed transalcoholysis of the *tert*-butyl ester groups of the PMMA-*b*-PtBA-*b*-PMMA precursors by *n*-butanol. Figure 1 shows the SEC traces for the first PMMA block, the PMMA-*b*-PtBA diblock, and the final MtBM triblock (sample 1 in Table 1). MWDs are monomodal and narrow ($M_w/M_n < 1.1$). Furthermore, the MW increases upon each step of the sequential block copolymerization, in good agreement with the values calculated from the monomer/initiator molar ratio. Monomer conversion is close to completion. The sequential polymerization is thus perfectly con-
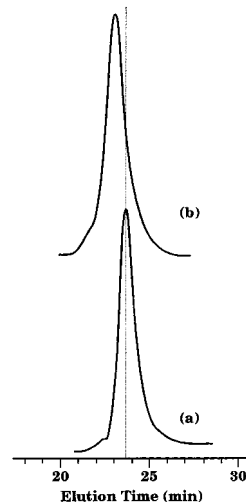
Figure 2. SEC traces of (a) PnBA macroinitiator and (b) MnBM triblock prepared by ATRP.

trolled, which is consistent with the living character of each step and the suitable cross-reactivity of the monomers. The MtBM precursor has been converted into the MnBM triblock by the acid-catalyzed transalcoholysis of the PtBA block by *n*-butanol. This reaction is selective in the presence of PMMA.[14] ^{1}H NMR analysis of the original MtBM and the final MnBM copolymers shows that tBA groups can no longer be detected in MnBM, although a very small part of these groups (2−5%) has been hydrolyzed rather than transalcoholyzed. Figure 1 shows that transalcoholysis of MtBM (sample 1) into MnBM does not change the MWD significantly. It may thus be concluded that fully acrylic analogues of the traditional TPEs of the SBS type can be tailored by sequential anionic polymerization of MMA and tBA, followed by selective transalcoholysis of the PtBA central block into a low-T_g PnBA block, as recently confirmed by Varshney et al.[15]

Radical Synthesis of MnBM Triblock by ATRP. A previous paper reported on the potential of NiBr$_2$-(PPh$_3$)$_2$ as catalyst for the ATRP of (meth)acrylic monomers[16] with the purpose to synthesize a MnBM triblock. Diethyl *meso*-2,5-dibromoadipate has proved to be an excellent initiator for the nBA polymerization, so leading to well-controlled monodisperse polymer ($M_w/M_n = 1.11$, Figure 2a), end-capped by a bromide at each chain end.[16] These bromide end groups are stable enough to survive in the further stage of purification and storage.[17] The nBA polymerization must however be stopped below 80% conversion, since a coupling reaction responsible for a shoulder on the high-MW side of the elution peak (Figure 2a) appears at high monomer conversion (80%) and increases with it. The recovered α,ω-bromo-PnBA can be used as macroinitiator for the synthesis of MnBM triblocks.[7] Figure 2b illustrates the SEC trace of the MnBM triblock copolymer and the distinct shift of the SEC trace of polynBA toward higher MW in agreement with the occurrence of block copolymerization. The SEC trace of the MnBM is monomodal although slightly broader than the MWD of the MnBM triblock synthesized by LAP (comparison of Figures 1d and 2b). The molecular characteristics of the two copolymers are reported in Table 1 and confirm the difference in the MWD, which is higher by 10% when the triblock is synthesized by ATRP rather than by LAP. This observation might indicate that the crossover reaction from α,ω-bromo-polyacrylate to polymethacry-

Table 2. Characterization of Homo-PMMAs Synthesized by LAP and ATRP

sample	M_n ($\times 10^{-3}$)	M_w/M_n	tacticity[a]	T_g (°C)
3, LAP	8.5	1.08	79:19:2	115
4, LAP	10.0	1.05	80:20:0	120
5, LAP	20.0	1.05	79:19:2	126
6, ATRP	8.9	1.40	57:37:6	113

[a] Syndiotactic:heterotactic:isotactic.

late by ATRP is not ideal.[7,18] Recently, Sawamoto et al. reported that the structure of the initiator used in the ATRP of MMA had a strong influence on the MWD.[19] These authors concluded that steric congestion around the α-carbon (radical center) contributed to the stabilization of the carbon radical and thus to the control of the ATRP. For example, they found that H(MMA)$_2$Br was one of the best initiators to prepare PMMA with a narrow MWD (M_n = 10 300; M_w/M_n = 1.19). There might thus be some problem when α,ω-Br-PnBA is used to initiate the MMA polymerization, since the α-carbon of the polyacrylate macroinitiator is not substituted. This question has been addressed by using diethyl *meso*-2,5-dibromoadipate, which mimics the poly(nBA) macroinitiator, as initiator for the MMA polymerization. Table 2 compares the molecular characteristics of PMMA samples prepared by LAP (samples 3−5) and by ATRP (sample 6). It is clear that the MWD of PMMA initiated by a bromide of the acrylic type is broader than the samples synthesized by LAP. One reason for the slow initiation of MMA by brominated polynBA macroinitiator might be found in the position of the equilibrium between dormant and active species, which is around 300 times more favorable to the reactive species in the case of MMA compared to nBA.[16] Therefore, although the apparent MWD of MnBM prepared by ATRP is narrow, the MWD of the short PMMA outer blocks (8000 compared to 50 000 for PnBA) might be broad. This expectation has been confirmed by experiments reported elsewhere.[7,18]

Characterization of MnBM Triblock Prepared by LAP and ATRP. Preliminary experimental data by DSC and NMR are reported in Table 1. In addition to similar values in MW, MWD, and PMMA content, the T_g's of both the PMMA outer blocks and the PnBA central block are essentially the same whatever the polymerization technique. From Table 2, it appears, however, that the PMMA tacticity is somewhat different when the synthesis conditions are changed (LAP vs ATRP), but not to the point where T_g is significantly modified.

Dynamic Temperature Sweep. Figures 3 and 4 compare the dynamic mechanical properties of the two types of triblock copolymers. It is clear that the T_g of the PnBA central block is identical. However, the modulus of the rubbery plateau is 1 decade higher when the triblock is synthesized by LAP rather than by ATRP (Figure 3), and the tan δ curve for the ATRP sample shows a very broad transition in the 0−80 °C temperature range (Figure 4). This substantial difference in the linear viscoelastic properties could be explained by the differences in macroscopic morphological orientations and/or in morphological details directly related to the molecular structure. As will be explained in the next section, the phase morphology of the bulk material cannot be directly observed by transmission electron microscopy (TEM) which is a serious limitation. Nevertheless, the two copolymers of same composition and
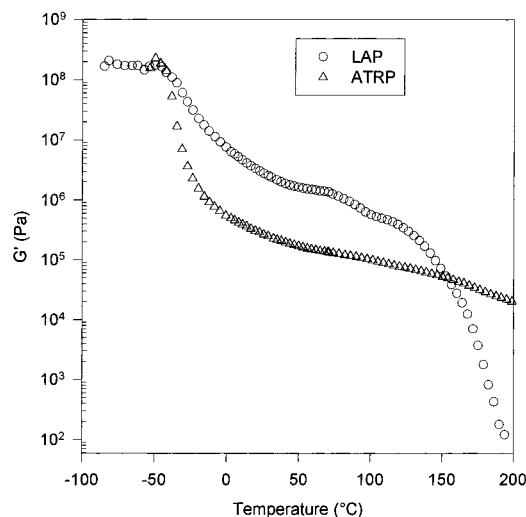
Figure 3. Storage modulus as a function of temperature for MnBM prepared by LAP (○) and ATRP (△). Heating rate: 2 °C/min; 1 Hz.
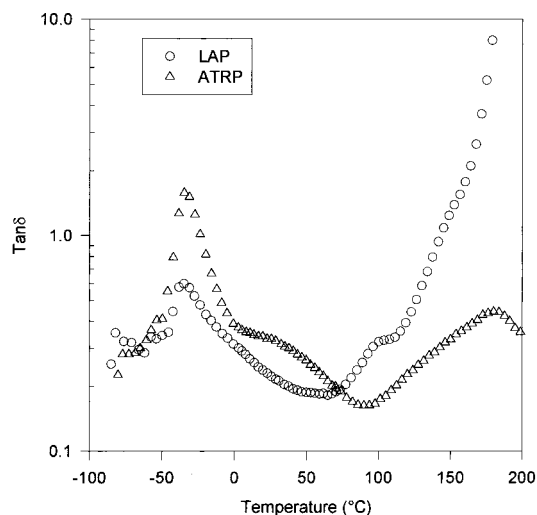
Figure 4. tan δ as a function of temperature for MnBM prepared by LAP (○) and ATRP (△). Heating rate: 2 °C/min; 1 Hz.

total molecular weight have been film-casted under the same experimental conditions and in a reproducible manner (reproducibility of the data in Figures 3 and 4). Therefore, the contribution of the molecular structure may not be ignored, particularly the unfavorable crossover reaction from acrylate to methacrylate in the ATRP synthesis. For this reason, the ATRP sample is thought to be a mixture of asymmetric triblocks as result of the broad MWD of the PMMA outer blocks. An indirect confirmation can be found in the broad intermediate maximum observed in the 0−80 °C temperature range of the tan δ curve for the ATRP sample (Figure 4), which might be assigned to dangling chains in the network, by analogy with the same transition observed for binary blends of triblock and diblock (or homopolymer), e.g., blends of polystyrene-*b*-polyisoprene-*b*-polystyrene triblock and polystyrene-*b*-polyisoprene diblock[20] and polystyrene-*b*-polybutadiene-*b*-polystyrene triblock and polybutadiene homopolymer.[21] The mechanism that sustains this broad transition has been studied by Berglund and Mckay.[20] It would originate from the relaxation of nonconstrained chains throughout the entangled rubbery matrix. In addition to MnBM triblocks, PMMA-*b*-poly(isooctyl acrylate)-*b*-PMMA (MIM)
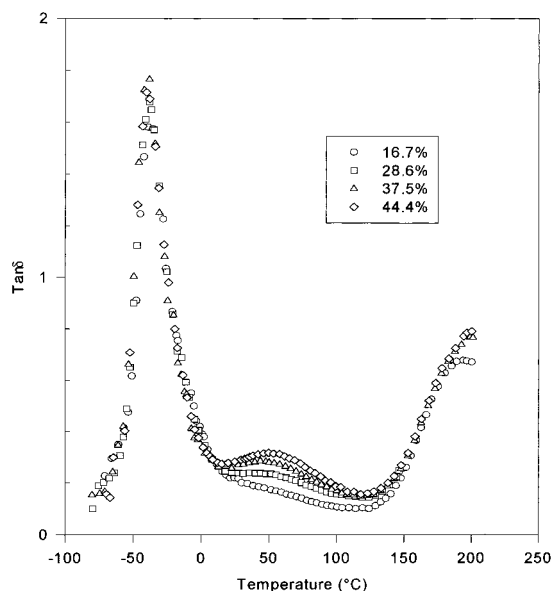
Figure 5. tan δ as a function of temperature for PMMA-*b*-PIOA-*b*-PMMA (10K-140K-10K) containing increasing amounts of PMMA-*b*-PIOA (10K-140K).

copolymers have also been synthesized by LAP, and their dynamic mechanical properties have been analyzed as shown in Figure 5. When these triblocks are contaminated by increasing amounts of parent diblocks, the temperature dependence of tan δ shows that an additional broad relaxation appears at ca. 50 °C and increases in intensity. It can only be explained by the relaxation of dangling poly(isooctyl acrylate) chains, which gives credit to the analysis of Figure 4 and to the hypothesis that part of the MnBM triblock chains are not part of the rubbery network. It may be noted here that the assignment of this intermediate maximum to the β relaxation in PMMA may be disregarded, since the height of the maximum increases when more diblock is added and thus when the PMMA content is decreased. Consistently, the G' modulus of the plateau region (~25−150 °C) decreases with increasing amount of diblock.

An additional striking difference between the LAP and the ATRP copolymers is that the flow regime which is expectedly observed above T_g of the PMMA microdomains (vide infra) in the LAP copolymer is not yet effective at 200 °C for the ATRP sample (Figure 3). The relaxation characteristic of this T_g is clearly observed in Figure 4 (at ca. 100 °C) although in partial overlap with the viscous response at higher temperature. In contrast, the ATRP copolymer shows only one very broad transition above ca. 90 °C, which might, however, result from the overlap of two individual ones (Figure 4). It has been reported that a sharp decrease in G' is observed at or near to the order−disorder transition temperature (T_{ODT}) of block copolymers when dynamic temperature sweeping experiments are conducted at low angular frequencies.[22−26] Therefore, Figures 3 and 4 indicate that the microphase-separated morphology of the LAP copolymer (vide infra) becomes disordered beyond ca. 120 °C, in contrast to the ordered phase-separated structure of the ATRP sample that persists at least up to 200 °C. It is generally accepted that in phase-separated block copolymers T_{ODT} is influenced by several factors, such as f (volume fraction), N (overall degree of polymerization), and χ (Flory−Huggins interaction parameter of the blocks) and that it increases as

N and χ are increased.[27] In the case of the ATRP triblock, the higher T_{ODT} is an indication for longer PMMA chains and thus for higher N and χ values.[28,29] This conclusion is consistent with the broader MWD for the outer PMMA blocks in the ATRP sample, as confirmed by homo-PMMA prepared by ATRP rather than by anionic process. The choice of the MW of the PMMA blocks is thought to be at the origin of the big differences observed in the behavior of the two MnBM triblocks at high temperature. The average MW between PMMA chain entanglements (6000) with respect to the MW of the PMMA blocks may have a drastic effect on the flow of the triblocks in the melt.

Characterization of the Phase Morphology. As mentioned elsewhere,[31] the lack of electronic contrast between the poly(alkyl acrylate) and poly(alkyl methacrylate) blocks and the problem raised by the selective staining of these constituents makes the direct observation of the bulk morphology impossible by TEM. Actually, AFM is the only experimental technique able to discriminate the two phases, although it provides information on the surface structure. Figure 6 compares the phase images recorded by the tapping-mode atomic force microscopy (TMAFM) for thin films of the LAP copolymer (Figure 6a) and ATRP sample (Figure 6b). It must be noted that the topographic images (not shown here) are featureless, indicating that the surface of the films is very smooth, the roughness being of a few nanometers. When the interaction between the tip and the material probed on the surface changes, the phase of the oscillating tip changes accordingly. It has been shown[11] that the phase lag is directly related to the elastic modulus of the material when the amplitude is only slightly dampened upon contact with the surface. (In this study, the damping was ca. 5%.) Therefore, the pattern of bright and dark areas on the phase images is the signature of microphase separation between the blocks. The brighter zones, characteristic of larger phase shifts, are assigned to the high-modulus thermoplastic domains of PMMA, and the darker areas (smaller phase shifts) are typical of the softer PnBA component.

The phase morphology expected for block copolymers that contain ca. 25 wt % of PMMA is an assembly of cylinders of PMMA into the matrix formed by the major component.[30] The LAP sample (Figure 6a) actually shows a complex pattern of bright cylinders (PMMA) in a darker continuous PnBA matrix. Most of these cylinders are somewhat elongated on the surface, with no specific orientation. Some of them appear as bright dots. The morphology of the ATRP sample (Figure 6b) is markedly different, since all the PMMA domains are round-shaped and they are assembled in a rather regular fashion. They are locally arranged in a hexagonal lattice. Actually, these domains are cylinders standing perpendicular to the surface, so that only their apex can be seen. If films of the ATRP copolymer are prepared with fast solvent evaporation, the surface morphology then consists of a mixture of cylinders lying flat on the surface and cylinders standing perpendicular to it.[31] The thermal annealing (at 140 °C for 24 h) of these films followed by slow cooling results in the morphology shown in Figure 6b. Nevertheless, the same thermal treatment does not lead to the same ordered morphology when the LAP sample is concerned.

The length of the cylinders seen in the surface in Figure 6a is not the actual full length of these objects. The major part of the cylinders is more likely immersed
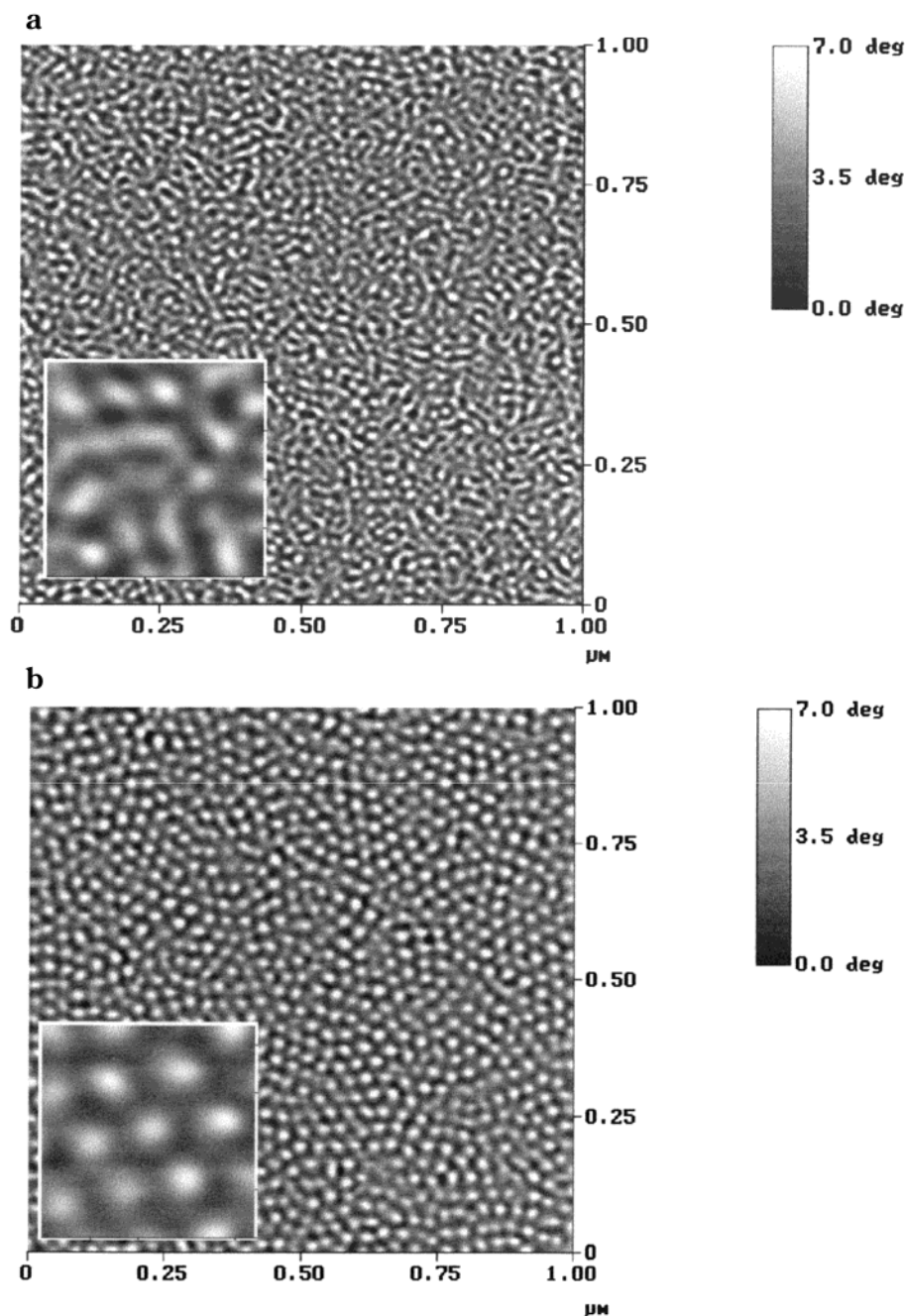
Figure 6. The 1 μm $\times$ 1 μm TMAFM phase images of the LAP sample (a) and ATRP sample (b). The insets are 110 nm $\times$ 110 nm zooms. The vertical scale is 7 deg.

in the bulk of the films. This segregation of the PMMA domains away from the surface is complete in Figure 6b, where only the apex of the cylinders is observed. This general behavior is thought to be driven by the difference in surface energy between PMMA and PnBA, which is responsible for the surface depletion in the most polar component.

Another major difference between the two images is the distance between the neighboring cylinders: the bright areas appear to be larger and at longer distance from each other in the ATRP sample compared to the LAP sample. This observation has been confirmed by the statistical analysis of the images, based on the power spectra density (PSD) analysis of the AFM images. PSD is currently a powerful tool to analyze the surface roughness and morphology of thin organic films.[32−34] It is calculated by integrating the Fourier

transform of the topographic profile over spatial frequencies characteristic of increasing length scales (from the interpixel distance to the full size of the image). From a single image, this approach thus allows the roughness to be estimated on different length scales. The application of this formalism to the AFM phase images is a way to know how the "phase roughness" (or "compositional roughness") changes with the length scale. Figure 7 shows the PSD curves extracted from the images of Figure 6. Starting from the short lengths, the PSD curves rapidly increase and then reach a plateau. This plateau indicates saturation of the roughness; thus, rougher features are unlikely to be found, even when exploring a much larger area. Most importantly, the length at the intersection between the plateau and the steep part of the curve is the correlation length typical of the surface, i.e., the characteristic
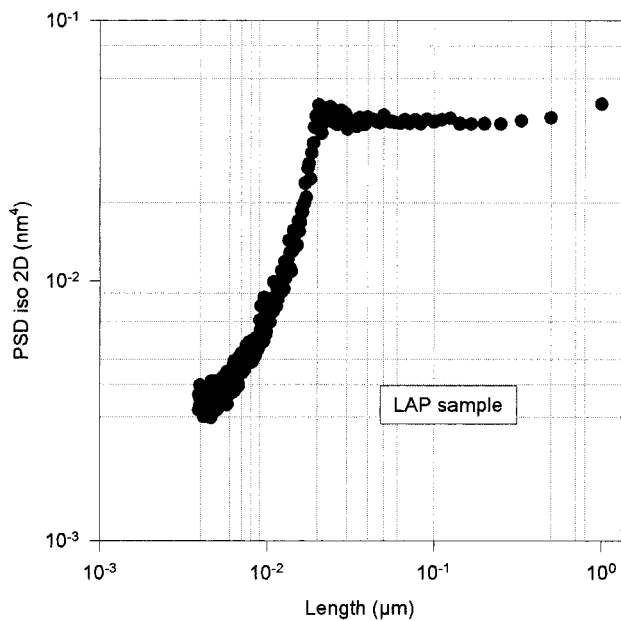
(a)
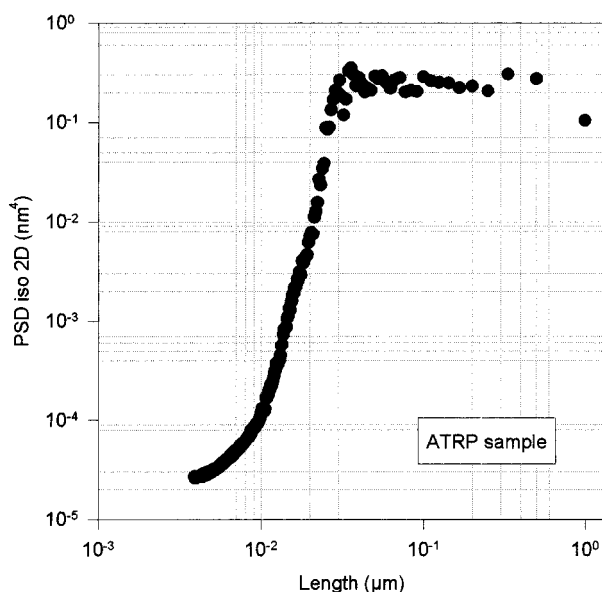
(b)

Figure 7. Two-dimensional PSD curves derived from the phase images of Figure 6: LAP sample (a) and ATRP sample (b).

distance between the top of two "hills" or the bottom of two "valleys" in the phase image. It clearly appears that the correlation length is ca. 20 nm in Figure 7a (LAP sample) and close to 30 nm in Figure 7b (ATRP sample). These figures confirm that the cylinders in Figure 6b are larger and located further away from each other the cylinders in Figure 6a.

This difference can be rationalized by the MWD of the PMMA blocks, which is much broader in the ATRP sample than in the LAP copolymer. The shortest PMMA blocks of the ATRP copolymer are more likely miscible to the PnBA matrix, which may result in slightly less phase separation surrounded by a more diffuse interface. It might also be argued that the chains that do not contribute to the physical stabilization tridimensional network can make the kinetics of microphase separation faster, such that the equilibrium morphology
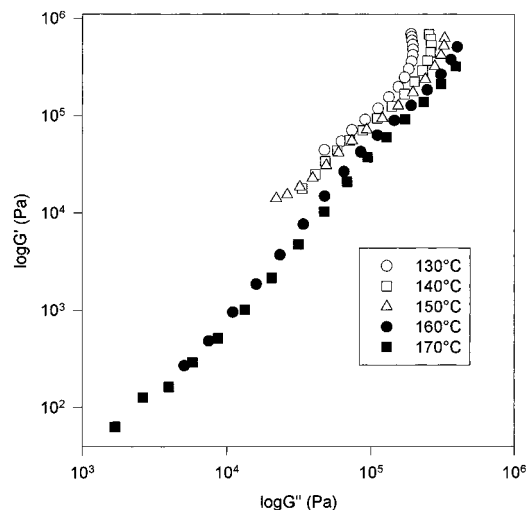
Figure 8. log G' vs log G'' for MnBM prepared by LAP (sample 1), at different temperatures.

would be observed for the ATRP copolymer and not for the LAP sample.

Dynamic Frequency Sweep. The end use of triblock copolymers as TPEs requires not only the physical stabilization of a tridimensional network of rubbery chains but also a processing temperature compatible with the thermal stability of the constitutive blocks. Triblocks cannot be processed properly at temperatures below the order–disorder transition temperature (T_{ODT}). Han and co-workers[22,35] have recently reported that T_{ODT} could be inferred from rheological measurements as illustrated in Figure 8 and thus from the log G' vs log G'' plots recorded at different temperatures. These authors have proposed that T_{ODT} is the threshold temperature at which the log G' vs log G'' plot becomes linear with a slope of 2 independent of the temperature. This prediction is based on eq 3, which is applicable to homogeneous polymers in the terminal viscoelastic zone:[22]

$$\log G' = 2 \log G'' - \log(\rho RT/M_e) + \log(\pi^2/8) \quad (3)$$

where ρ is the polymer density, R the gas constant, T the temperature, and M_e the average MW between chain entanglements. Figure 8 shows that the log G' vs log G'' data overlap at temperatures of 160 °C and higher, which is accordingly the T_{ODT} of the LAP triblock. Figure 9 illustrates the same dependence for the ATRP triblock and shows that the log G' vs log G'' plots do not overlap each other and fail to comply with a linear relationship even at 200 °C. Therefore, the T_{ODT} is beyond this upper investigated temperature. Figure 10 shows how the complex viscosity depends on the angular frequency for the LAP triblock at different temperatures. The complex viscosity at and below 150 °C is typically non-Newtonian as is for instance the case for vulcanized rubbers. A yield behavior is, however, observed at 160 °C together with a Newtonian behavior at low shear rate, which is in possible relation to the ODT. The Newtonian behavior becomes more pronounced with higher temperature and extends over the whole investigated frequency range at 200 °C. The same plots as in Figure 10 are reported for the ATRP sample in Figure 11. The conclusions are here completely different, since the complex viscosity is typically non-Newtonian in the whole investigated temperature and
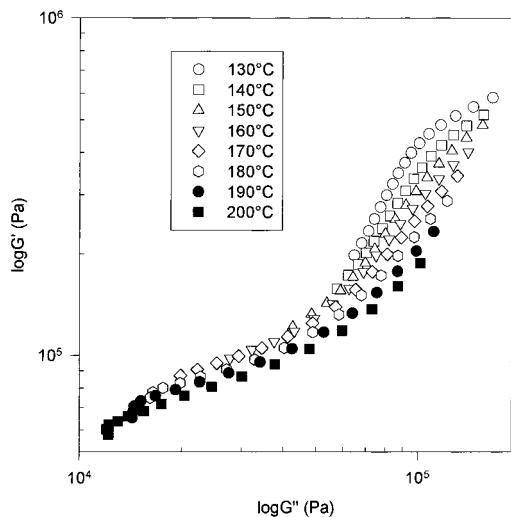
Figure 9. log G' vs log G'' for MnBM prepared by ATRP (sample 2), at different temperatures.
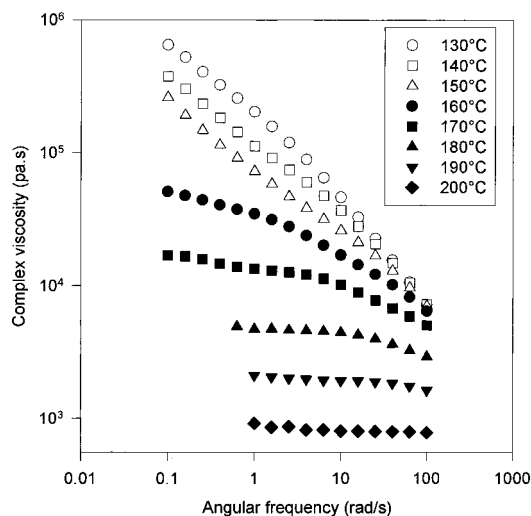
Figure 10. Complex viscosity as a function of angular frequency for MnBM prepared by LAP (sample 1), at different temperatures.
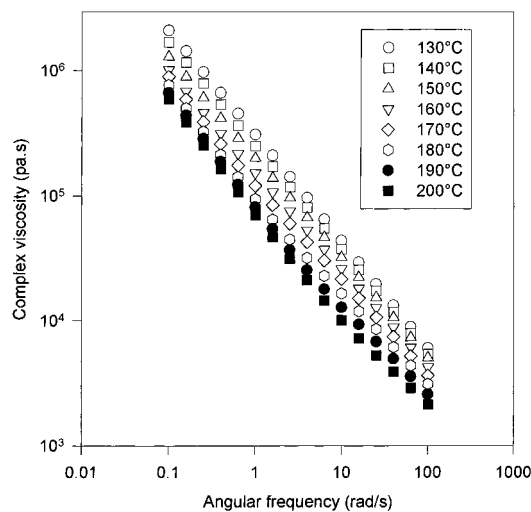
Figure 11. Complex viscosity as a function of angular frequency for MnBM prepared by ATRP (sample 2), at different temperatures.

frequency ranges (Figure 11). It is thus clear that T_{ODT} for the ATRP sample is much higher than for the LAP sample, which raises the question of the processing of
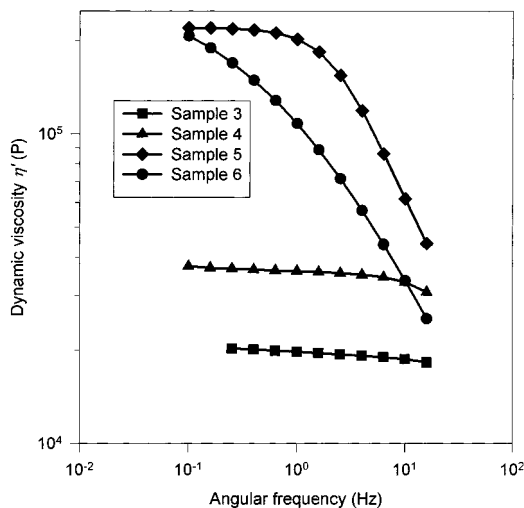
Figure 12. Dynamic viscosity (η') as a function of angular frequency at 180 °C for PMMA prepared by LAP (samples 3–5) and ATRP (sample 6).

this triblock. To confirm that the broader MWD of the PMMA blocks of the ATRP sample is the origin of the observed discrepancy, the dynamic viscosity has been measured at 180 °C for four PMMA samples synthesized by LAP (samples 3, 4, 5; Table 2) and ATRP (sample 6; Table 2) (Figure 12). For the anionically prepared PMMA samples of narrow MWD, distinct Newtonian and non-Newtonian regimes are observed in relation to MW and shear rate. At comparable MW, although the LAP samples (3 and 4; Table 2) are Newtonian at 180 °C, the ATRP sample is typically non-Newtonian and behaves much like the LAP sample (sample 5; Table 2) of 2 times higher MW. This observation again empha-sizes the critical role of polydispersity, since an increase in polydispersity from ca. 1.05 to 1.4 is enough to change dramatically the viscoelastic properties with PMMA of the same MW. This difference is compensated with the 2 times increase in MW of PMMA sample of narrow MWD. The effects of MWD on the viscoelastic properties are well-known[36] and explained by the broadening of the relaxation time distribution as the polydispersity is increased. The zero-shear viscosity, η_0, of polydisperse polymers appears to depend on M_t, which lies between M_w (weight-average MW) and M_z (*z*-average MW), although being close to M_w in the case of low polydis-persity and approaching M_z as the polydispersity is higher.[37,38] Compared to the LAP samples (3 and 4) with the same M_n, the ATRP sample 6 has higher M_w and M_z and consequently higher η_0. As a result of the polydispersity issue, the flow of radically made PMMA is thus kinetically less favorable, this kinetic restriction being at the origin of the apparent discrepancy shown by the viscoelastic behavior of LAP and ATRP triblock copolymers.

Tensile Behavior. Figure 13 compares the stress–strain behavior for the two triblocks. Although both of them behave as a vulcanized elastomer, some distinct differences deserve comments. First, the initial modulus of the LAP sample is much higher compared to the ATRP one. Second, the ultimate tensile strength and elongation at break are much higher for the LAP sample than for the ATRP counterpart. Finally, the tensile strength of the LAP triblock slows down before sample breaking. The first two differences are consistent with the only partial contribution of the ATRP triblock to the chain network. The third observation more likely results
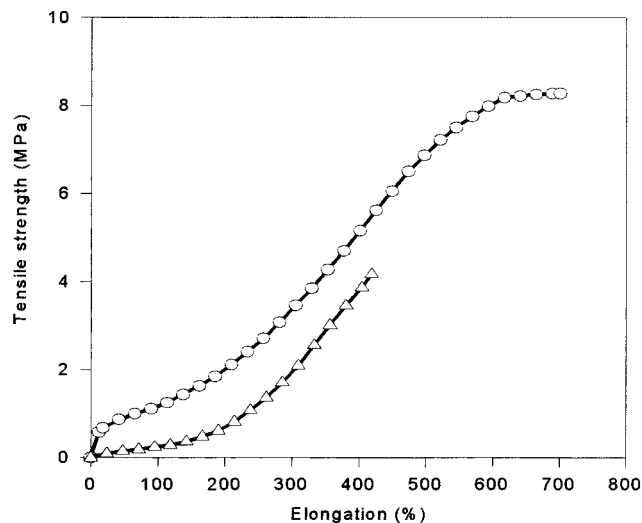
Figure 13. Stress−strain curves for MnBM prepared by LAP (○) and ATRP (△).

from the relatively low MW of the PMMA outer blocks, so that part of them can be pulled out of the microdomains before the sample breaks down.

Conclusions

We have reported the synthesis and characterization of two poly(methyl methacrylate)-*b*-poly(*n*-butyl acrylate)-*b*-poly(methyl methacrylate) triblock copolymers (MnBM), prepared by ligated anionic polymerization and atom transfer radical polymerization. The molecular characteristics of the two triblocks are essentially the same, except for the MWD of the PMMA outer blocks which is broader for the ATRP sample. The LAP system exhibits the typical behavior of thermoplastic elastomers in relation to perfectly controlled molecular structure. In contrast, due to PMMA outer blocks of uneven length, part of the ATRP triblock chains (those ones containing at least one very short PMMA block) most likely do not participate in the network formation, thereby leading to low storage modulus and poor ultimate tensile properties. The AFM observations confirm that the phase separation occurs in the two copolymers and that the same cylindrical morphology is developed although with different periodicity and orientation. This difference in morphology is the consequence of the shortest PMMA outer blocks in the ATRP copolymers, which allow the phase separation to reach equilibrium (cylinders perpendicular to the film surface) and to form slightly less cylinders surrounded by more diffuse interface. The triblock chains that are in the ATRP compound contain outer PMMA blocks of higher M_w and M_z and are responsible for the higher complex viscosity and order−disorder transition temperature of the ATRP copolymer compared to the LAP triblock. Therefore, although the ATRP technique has the advantage of simple and mild polymerization conditions, the molecular control of the final product is not stringent enough for fully (meth)acrylic triblock copolymers to exhibit the ideal behavior of thermoplastic elastomers. Effort is now devoted to decreasing the polydispersity of the PMMA outer blocks in triblocks prepared by controlled radical polymerization.[39]

References and Notes

(1) Jérôme, R.; Bayard, Ph.; Fayt, R.; Jacobs, Ch.; Varshney, S.; Teyssié, Ph. In *Thermoplastic Elastomers,* 2nd ed.; Holden, G., Legge, N. R., Quirk, R., Schroeder, H. E., Eds.; Hanser: Munich, 1996; p 521.

(2) Arehart, S. V.; Greszta, D.; Matyjaszewski, K. *Polym. Prepr.* **1997**, *38*, 705.

(3) Ueda, J.; Matsuyama, M.; Kamigaito, M.; Sawamoto, M. *Macromolecules* **1998**, *31*, 557.

(4) Matyjaszewski, K.; Gaynor, S. G. *Macromolecules* **1997**, *30*, 7042.

(5) Cowie, J. M. G.; Ferguson, R.; Fernandez, M. D.; Fernandez, M. J.; McEwen, I. J. *Macromolecules* **1992**, *25*, 3170.

(6) Tong, J. D.; Jérôme, R. *Polymer*, in press.

(7) Moineau, G.; Minet, M.; Teyssié, Ph.; Jérôme, R. *Macromolecules*, in press.

(8) Benoit, S. K.; Grudissic, Z.; Rempp, P.; Decker, P.; Zilliox, J. *J. Chim. Phys.* **1966**, *63*, 1507.

(9) Taquet, A. Master thesis, University of Liège, Belgium, 1990.

(10) Penzel, E.; Goetz, N. *Angew. Makromol. Chem.* **1990**, *178*, 191.

(11) (a) Leclère, Ph.; Lazzaroni, R. Brédas, J. L.; Yu, J. M.; Dubois, Ph.; Jérôme, R. *Langmuir* **1996**, *12*, 4317. (b) Bar, G.; Thomman, Y.; Brandsch, R.; Cantow, H. J.; Whangbo, M. H. *Langmuir* **1997**, *13*, 3807. (c) Magonov, S. N.; Elings, V.; Whangbo, W. H. *Surf. Sci. Lett.* **1997**, *375*, L385. (d) Burnham, N. A. Behrend, O. P.; Oulevey, F.; Gremaud, G.; Gallo, P.-J.; Gourdon, D.; Dupas, E.; Kulik, A. J.; Pollock, H. M.; Briggs G. A. D. *Nanotechnology* **1997**, *8*, 67.

(12) Nugay, N.; Nugay, T.; Jérôme, R.; Teyssié, Ph. *J. Polym. Sci., Part A* **1997**, *35*, 361.

(13) Nugay, N.; Nugay, T.; Jérôme, R.; Teyssié, Ph. *J. Polym. Sci., Part A* **1997**, *35*, 1543.

(14) Deporter, C. D.; Long, T. E.; McGrath, J. E. *Polym. Int.* **1994**, *33*, 205.

(15) Varshney, S. K.; Kesani, P.; Agarwal, N.; Zhang, J. X. *Macromolecules* **1999**, *32*, 235.

(16) Moineau, G.; Minet, M.; Dubois, P.; Teyssié, P.; Senninger, T.; Jérôme, R. *Macromolecules* **1999**, *32*, 27.

(17) Nishikawa, T.; Ando, T.; Kamigaito, M.; Sawamoto, M. *Macromolecules* **1997**, *30*, 2244.

(18) Shipp, D. A.; Wang, J.-L.; Matyjaszewski, K. *Macromolecules* **1998**, *31*, 8005.

(19) Ando, T.; Kamigato, M.; Sawamoto, M. *Tetrahedron* **1997**, *53*, 15445.

(20) Berglund, C. A.; Mckay, K. W. *Polym. Eng. Sci.* **1993**, *33*, 1195.

(21) Choi, G.; Kaya, A.; Shen, M. *Polym. Eng. Sci.* **1973**, *13*, 231.

(22) Han, C. D.; Baek, D. M.; Kim, J. K.; Ogawa, T.; Sakamoto, N.; Hashimoto, T. *Macromolecules* **1995**, *28*, 5043.

(23) Winey, K. I.; Gobran, D. S.; Xu, Z.; Fetters, L. J.; Thomas, E. L. *Macromolecules* **1994**, *27*, 2392.

(24) Chung, C. I.; Lin, M. I. *J. Polym. Sci., Polym. Phys. Ed.* **1978**, *16*, 545.

(25) Bates, F. S. *Macromolecules* **1984**, *17*, 2607.

(26) Gehlsen, M. D.; Bates, F. S. *Macromolecules* **1993**, *26*, 4122.

(27) Leibler, L. *Macromolecules* **1980**, *13*, 1062.

(28) Tang, H.; Feed, K. F. *J. Chem. Phys.* **1992**, *96*, 8621.

(29) Dudowicz, J.; Freed, K. F. *Macromolecules* **1993**, *26*, 213.

(30) Bates, F. S.; Fredrickson, G. H. *Annu. Rev. Phys. Chem.* **1990**, *41*, 525.

(31) Leclère, Ph.; Moineau, G.; Minet, M.; Dubois, Ph.; Jérôme, R.; Brédas, J. L.; Lazzaroni, R. *Langmuir* **1999**, *15*, 3915.

(32) Krim, J.; Heyvaert, I.; Haesendonck, C. V.; Bruynseraede, Y. *Phys. Rev. Lett.* **1993**, *70*, 57.

(33) Biscarini, F.; Samorì, P.; Greco. O.; Zamboni, R. *Phys. Rev. Lett.* **1997**, *78*, 708.

(34) Viville, P.; Lazzaroni, R.; Brédas, J. L.; Moretti, P.; Samorì, P.; Biscarini, F.; *Adv Mater.* **1998**, *10*, 57.

(35) Han, C.; Kim, J. *J. Polym. Sci., Part B* **1987**, *25*, 1741.
(36) Ferry, J. D. *Viscoelastic Properties of Polymers,* 2nd ed.; Wiley: New York, 1970.
(37) Bueche, F. *J. Polym. Sci.* **1960**, *43*, 527.
(38) Graessley, W. W. *J. Chem. Phys.* **1967**, *47*, 1942.

(39) Moineau, G.; Minet, M.; Teyssié, Ph.; Jérôme, R., submitted for publication.

MA990886V